Applied Chemical Engineering (2025) Volume 8 Issue 4 ISSN: 2578-2010 (O)
doi: 10.59429/ace.v8i4.5818

ORIGINAL RESEARCH ARTICLE

Sequential combination of electrocoagulation and Electro-fenton for COD removal of real petroleum refinery wastewater

Murtada S. Khalaf[1*], Alaa N. Ghanim[2]

[12] *Chemical Engineering Department, College of Engineering, University of Babylon, Babil, 51002, Iraq*

***Corresponding author:** Murtada S. Khalaf; eng498.murtada.salam@student.uobabylon.edu.iq

ABSTRACT

Electrocoagulation (EC) and electro-Fenton (EF) are effective electrochemical methods utilized for the removal of organic pollutants from wastewater. Electrochemical techniques facilitate the removal of contaminants by metal dissolution., EF creates hydroxyl radicals (•OH) by reacting H_2O_2 with Fe^{2+}, facilitating advanced oxidation. This study treated the Najaf refinery, Iraq wastewater with a combination EC/EF procedure. The raw wastewater had an initial chemical oxygen demand (COD) of 700 mg/L. EC was conducted for 60 minutes at pH = 7 and room temperature using four iron electrodes (total active area: 100 cm²). The EF process was carried out for 120 minutes at a pH of 3 utilizing two porous graphite electrodes with an area of 60 cm² each. The experiments included variations in the current density (20–50 mA/cm²), hydrogen peroxide H_2O_2 concentration addition (0.5–2.0 g/L), and pH values. The combined system attained a maximum COD removal efficiency of 99.42% at 40 mA/cm² and 0.5 g/L H_2O_2 , validating the significant potential of this approach for industrial wastewater treatment.

Keywords: Electrocoagulation; Electro-Fenton ; COD ; Kinetics ; hydrogen peroxide

ARTICLE INFO

Received: 6 November 2025
Accepted: 11 December 2025
Available online: 24 December 2025

1. Introduction

Petroleum refinery wastewater is considered one of the most challenging industrial effluents due to its high content of refractory organic matter and toxic chemicals. Refining activities consume substantial quantities of water, producing effluents laden with hydrocarbons, phenols, sulfides, ammonia, suspended particles, and heavy metals. These pollutants lead to increased chemical oxygen demand (COD) and reduced biodegradability, presenting significant threats to aquatic ecosystems and public health if discharged untreated [1,2]. Some heavy metals, such as nickel, chromium, and lead, found in wastewater are known to cause severe biological toxicity. Studies have shown that these metals not only raise COD but also impair cell integrity and reproductive functions. This fact is evident in some studies that indicate the harmful effect of nanocrystals on sperm viability and mammalian fertility, as these crystals are arranged with heavy metals [3]Traditional treatment techniques—such as coagulation, flocculation [4], oxidation [5] biological oxidation ozonation [6], and membrane separation[7] .They have been widely used for wastewater treatment. However, these traditional processes usually show limited treatment efficiency for the highly resistant organic pollutants present in petroleum wastewater. Therefore, the need arises for the use of more integrated and effective treatment methods and techniques. Therefore, advanced processes are urgently required to ensure effective COD abatement from refinery effluents. Given that untreated refinery wastewater contributes to hydrocarbon-induced aquatic contamination, the development of efficient treatment strategies (such as EC/EF) supports international frameworks that emphasize liability, preventive control, and environmental stewardship in managing oil-related pollutants in marine environments [8] .

1.Electrochemical processes have emerged as promising technologies for industrial wastewater treatment, offering flexibility, environmental compatibility, and the potential for on-site generation of reactive species without significant chemical additives[9] . Among these, electrocoagulation (EC) and electro-Fenton (EF) have attracted growing interest for treating refinery and petrochemical effluents. EC relies on sacrificial metal electrodes (commonly iron or aluminum) to release coagulant species in situ, which destabilize colloids, adsorb dissolved organics, and promote electroflotation through hydrogen bubble generation. This process reduces turbidity, emulsified oils, and a significant fraction of COD, thereby improving the efficiency of subsequent treatments[10, 11] . On the other hand, the EF process is one of the most efficient advanced oxidation processes, producing hydroxyl radicals (•OH) through the reaction between electro-generated or externally added H_2O_2 and Fe^{2+} ions. These radicals are highly reactive and capable of mineralizing a wide spectrum of refractory organics into harmless end products such as CO_2 and H_2O [12,13]. There are also similar radical generation pathways during the processing of iron oxide nanoparticle systems with the help of iron, for example, $TiO_2/\alpha\text{-}Fe_2O_3$ photocatalyst thin films, which highlight the major role of iron and are based on the production of oxidizing species responsible for organic decomposition [14].

The integration of EC as a pretreatment with EF as a polishing step has recently been proposed as a synergistic approach for wastewater containing persistent organic pollutants[9]. EC reduces the pollutant load and removes radical scavengers, while EF subsequently degrades the remaining refractory fraction through advanced oxidation. Several recent studies have demonstrated that sequential EC/EF systems outperform standalone processes in terms of COD removal, reaction kinetics, and overall treatment efficiency[15 - 17] . This integrated strategy, therefore, provides a practical and scalable solution for refinery wastewater treatment, where both turbidity reduction and organic mineralization are required to meet discharge standards[1].

The principal responses implicated in the EC and EF processes are as follows [18]:

Anode (EC):

$$Fe\ (s) \rightarrow Fe^{2+} + 2e^- \qquad (1)$$

Cathode (EC – in alkaline medium):

$$O_2 + 2H_2O + 4e^- \rightarrow 4OH^- \qquad (2)$$

Formation of precipitate:

$$Fe^{2+} + 2OH^- \rightarrow Fe(OH)_2(s) \qquad (3)$$

Electro-Fenton reaction:

Fenton reaction:

$$Fe^{2+} + H_2O_2 \rightarrow Fe^{3+} + \bullet OH + OH^- \qquad (4)$$

Regeneration of Fe^{2+} at cathode:

$$Fe^{3+} + e^- \rightarrow Fe^{2+} \qquad (5)$$

Optional: in situ generation of H_2O_2:

$$O_2 + 2H^+ + 2e^- \rightarrow H_2O_2 \qquad (6)$$

Decomposition of H_2O_2 :

$$2H_2O_2 \rightarrow 2H_2O + O_2 \qquad (7)$$

Radical scavenging:

$$\bullet OH + \bullet OH \rightarrow H_2O_2 \tag{8}$$

Secondary reaction:

$$H_2O_2 + \bullet OH \rightarrow HO_2\bullet + H_2O \tag{9}$$

This study examined a two-step treatment process that sequentially applies EC/EF to enhance the removal of COD from refinery petroleum wastewater. The EC procedure served as a pretreatment step to reduce COD and enhance the effectiveness of the subsequent EF oxidation [9,19] . Experiments employed real wastewater sourced from the Najaf refinery in Iraq, utilizing iron and porous graphite electrodes. The effects of various current strengths and H_2O_2 levels were studied, and additional tests were done to see how pH affected the results under the best conditions. The necessity of adopting advanced treatment technologies such as the EC/EF system aligns with broader environmental management perspectives, where inadequate control of industrial effluents can impose indirect economic burdens on households and ecosystems, similar to the macro-environmental impacts observed in policy-driven agricultural subsidy reforms [20].

The novelty of this study lies in its use of real wastewater from oil refineries, which addresses some gaps in previous EC/EF studies that were not adequately addressed or resolved. Firstly, it utilized real wastewater from an Iraqi oil refinery (the Najaf Refinery), not artificial or simulated wastewater. This water has complex characteristics, including high levels of sulfates, phenols, resistant organic compounds, and high salinity. Consequently, the results provide a realistic assessment of the treatment efficiency. Secondly, the study analyzed the sludge formed after the electrocoagulation process, a crucial aspect often overlooked in EC/EF treatment. This analysis was enhanced by examining the residual sludge and determining its composition and proportions using SEM technology. Thirdly, the kinetics of both EC and EF processes were investigated, employing multiple models to elucidate the behavior of the two systems and gain a more thorough understanding of the removal mechanisms than is commonly found in some studies. Finally, an experimental design was developed that included a wider operational range, including studying variations in current densities, pH, and peroxide dosages added to the EF step, thus providing a greater understanding of process behavior. Overall, all these possibilities offered a realistic reflection of the mechanisms and behaviors through real-world mechanics, thereby enhancing existing knowledge in sequential EC/EF process studies using real complex wastewater.

2. Experimental work

2.1. Materials and methods

The present study involved collecting 30 liters of wastewater samples from the feeding tank to the treatment unit at the Najaf refinery in Iraq. This was done during a single operating cycle to avoid changes in properties and time variations. Mixing was maintained before sampling to prevent phase separation and ensure homogeneity of all samples. The collected sample was stored at 4°C to avoid daily variations in composition and was used for all experiments. Preliminary tests were performed before the start of the process, revealing no significant changes or fluctuations in key properties such as COD, pH, and oil content during storage. Therefore, a single batch of well-stored, controlled-condition wastewater from the refinery was used for all experiments. **Table 1** enumerates the diverse characteristics of wastewater. In each experiment, one liter of collected wastewater was filtered in two steps using a cotton filter and a CTO filter to remove pollutants, clay, and certain oils and greases before treatment. Sulfuric acid (H_2SO_4, 98%) and sodium hydroxide (NaOH, 5 M, 97%) from Thomas Indian Bakers were used to change the pH of the solution, which was checked with a microprocessor pH meter (HANNA, pH meter 211). Additionally, in each experiment, the iron electrodes were purified and activated by immersion in 5% (v/v) HCl for 10 minutes, followed by thorough rinsing with distilled water, and subsequently dried in an oven at 100°C to eliminate residual moisture. The electrodes were subsequently submerged in a 2.8% hexamethylenetetramine solution for 5 minutes.

Table 1. Petroleum wastewater properties.

Properties	Value
pH	7.7 – 7.9
TDS (mg/L)	3220-3280
Turbidity (NTU)	49-53
BOD (mg/L)	110-123
COD (mg/L)	690-710
Phenol (mg/L)	14.3 – 15.1
PO_4 (mg/L)	0.22 – 0.26
Cl^- (mg/L)	2200 - 2320
Oil (mg/L)	32 - 35

2.2. The apparatus

The experiments were performed at room temperature (25±5°C) in a batch monopolar electrochemical cell, as seen in **Figure 1**. The process was carried out inside a 1-liter glass cell. Subsequently, the cell was positioned on a magnetic stirrer at 250 rpm to get optimal mass transfer. The cathode electrodes in the EC process are two iron plates, whereas the anode electrodes are also two Fe plates, each with dimensions of 15 × 3.5 × 0.2 cm and an effective surface area of 100 cm^2. In the EF process, two plates of porous graphite were used as an anode and the other as a cathode, each with dimensions of 15 × 6 × 0.3 cm and an effective surface area of 60 cm^2. A DC power supply (0–30 V, 0–5 A) was used to regulate the electrical input during the experiments. Voltage and current were monitored and controlled using a digital voltmeter and a multimeter, respectively. Additionally, a pH probe equipped with a thermometer (HANNA, pH 211) was used to measure and monitor the pH and temperature of the solution throughout the experiments. The interelectrode gap was maintained at 1.5 cm between them, the effective area of the irons and porous graphite electrodes was calculated.

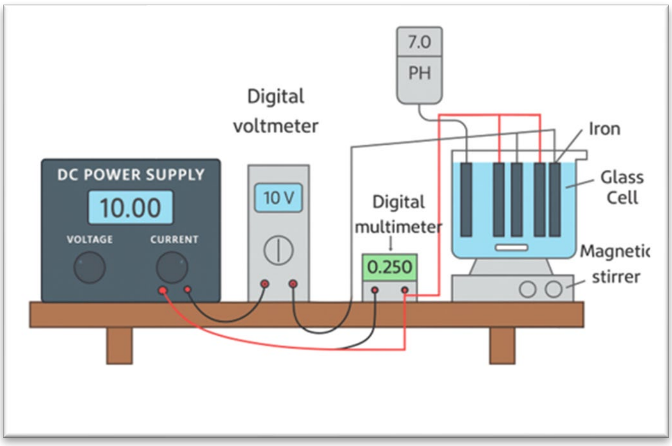

Figure 1. Experimental setup of the EC/EF process.

2.3. The method

The electrocoagulation procedure was performed in a 1-liter glass reactor fitted with four parallel iron electrodes (comprising two anodes and two cathodes). The electrodes were connected to a DC power source, and the reaction was conducted for one hour and a pH of 7. After the end of the EC process, the treated solution was subjected to filtration through a 0.45 μm filter paper to eliminate suspended particles and flocs. Thereafter, the iron electrodes were substituted with two porous graphite plates (one serving as the anode and the other as the cathode), and the electro-Fenton (EF) process commenced. The EF procedure was conducted at pH=3 for 2 hours under identical mixing circumstances. Different current densities (20, 30, 40, and 50 mA/cm²) and hydrogen peroxide H_2O_2 addition (0.5, 1.0, 1.5, and 2.0 g/L) were used. Four distinct H_2O_2 addition were examined for each current density. pH levels (1, 3, 5, and 7) were tested under the best EC/EF conditions to assess their effect on COD removal efficiency.

2.4. COD analysis

The concentrations of COD were quantified at the Environmental Engineering Laboratory, College of Engineering, University of Babylon, using a Lovibond MD 200 COD Vario photometer. Measurements were conducted at varying time intervals: every 15 minutes for the EC process and every 30 minutes for the EF process. The effectiveness of COD removal was determined using the following equation:

$$COD_{Removal}\% = \frac{COD_o - COD_t}{COD_o} \times 100$$

Where: COD_o is the initial COD concentration, and COD_t is the COD concentration at time t. The initial COD value was measured as 700 mg/L.

3. Results and discussion

3.1. Effect of current density

The current density is a crucial operational parameter that profoundly influences the efficacy of electrochemical treatment techniques. During the electrocoagulation (EC) step, an increase in current density expedites the anodic dissolution of sacrificial iron electrodes, leading to a greater production of coagulant species and augmented bubble creation, which promote the destabilization and aggregation of pollutants [2, 21]. In the electro-Fenton (EF) step, an increased current density enhances the generation of hydroxyl radicals (•OH), which are the primary oxidizing agents responsible for the breakdown of organic pollutants [22, 23]. Recent experimental findings strongly corroborate these observations, indicating that ideal current density levels enhance treatment efficacy, whereas excessively high values may result in adverse side reactions, such as peroxide breakdown or energy inefficiency [2,23]. The research indicated that the ability to remove COD enhanced markedly as the current density increased from 20 to 50 mA/cm², achieving a maximum efficiency of 99.42% at 40 mA/cm² with 0.5 g/L H_2O_2 addition. This improvement is mainly due to the simultaneous increase in the excess of electro-generated coagulants and oxidative radical generation. A slight decline in performance was noted at 50 mA/cm². Such a drop may result from parasitic side reactions, primarily oxygen evolution and rapid decomposition of H_2O_2 and the formation of less reactive species, which collectively diminish the availability of •OH radicals [21-24]. Also, higher current densities can cause the electrodes to become less effective and reduce the system's current (Faradaic) efficiency, due to energy losses associated with undesired side reactions, electrode passivation, and thermal effects [17,18]. **Figure 2** shows the variation of COD removal efficiency over time at a constant current density of 40 mA/cm² across various H_2O_2 additions. It was noted that raising the H_2O_2 dose addition above 0.5 g/L resulted in a minor decrease in COD removal efficiency, suggesting that an excess of peroxide may facilitate scavenging reactions that decrease oxidation efficacy.

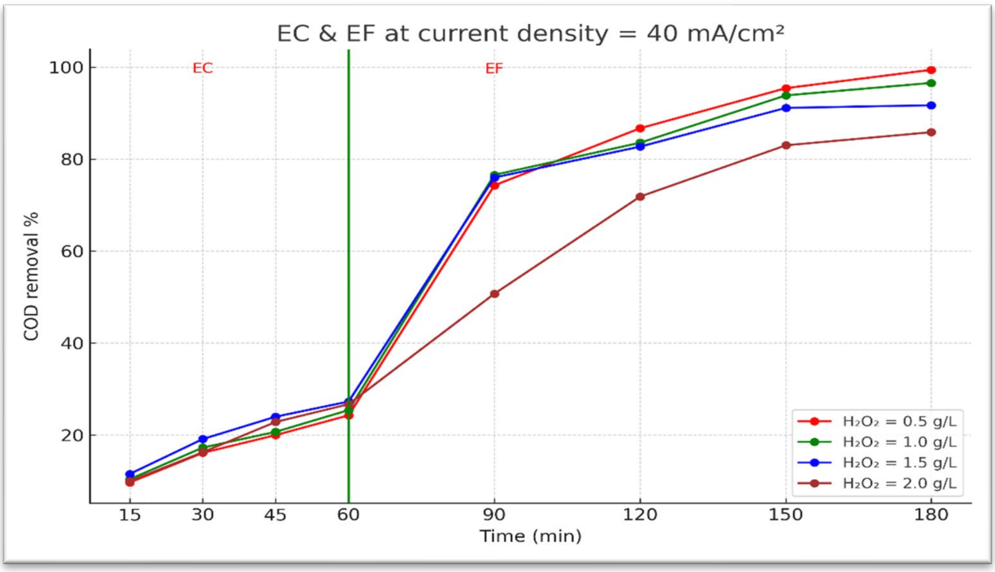

Figure 2. COD removal efficiency vs. time with different [H_2O_2] addition, condition: pH = 7; concentration = 4170 mg/L; current density = 40 mA/cm^2.

Table 2 presents a comparison of the performance of some literature, similar to the EC/EF electrochemical process.

Table 2. COD removal performance in EC/EF systems for some literature.

Study	Wastewater Type	EC/EF Configuration	COD Removal (%)	Reference
Agarwal et al. (2024)	Synthetic textile wastewater	EC → EF	93.20%	[19]
Chithra et al. (2010)	Textile effluent	EC → EF	88–94%	[25]
Akyol et al. (2013)	Fertilizer plant wastewater	EC → EF	72–85%	[26]
Nidheesh et al. (2022)	Mixed industrial wastewater	EC → Heterogeneous EF	85.27%	[27]
Gökkuş et al. (2023)	Dye-bearing wastewater	EC → EF	78–90%	[9]

3.2. Effect of H_2O_2 addition

The concentration of hydrogen peroxide H_2O_2 is essential for the efficacy of the electro-Fenton (EF) process, as it influences the availability of hydroxyl radicals (•OH), which are the primary agents responsible for reducing chemical oxygen demand (COD). This investigation achieved optimal COD removal at 0.5 g/L of H_2O_2 combined with a current density of 40 mA/cm², yielding a maximum removal efficiency of 99.42%. A slight increase to 1.0 g/L sustained exceptional performance; however, further increments to 1.5 and 2.0 g/L resulted in a substantial decline in oxidation efficiency. This decrease can be ascribed to the surplus H_2O_2 functioning as a scavenger of •OH radicals[28]. At heightened peroxide concentrations, adverse reactions become significant, such as :

$$H_2O_2 + \bullet OH \rightarrow H_2O + HO_2\bullet \qquad (10)$$

This reaction creates hydroperoxyl radicals ($HO_2\bullet$), which are considerably less reactive than hydroxyl radicals (•OH), thereby diminishing the system's overall oxidation capacity. Moreover, elevated concentrations of H_2O_2 can lead to parasitic Fenton-type side reactions such as scavenging of Fe^{2+} by H_2O_2 that deplete the available catalyst for •OH generation, ultimately reducing oxidative efficiency [24, 29]. Prior research has shown that elevated concentrations of H_2O_2 can impede the efficacy of the Fenton and electro-Fenton processes by scavenging hydroxyl radicals (•OH). It is essential to sustain an appropriate H_2O_2/Fe^{2+} molar ratio to maximize

COD removal and avert radical quenching [30] .Elevated H_2O_2 concentrations can lead to parasitic Fenton-type side reactions, such as consuming Fe^{2+}—which in turn reduces the availability of catalysts needed for continuous •OH generation. Consequently, the results indicate that preserving an optimal H_2O_2 dosage is important for ensuring an effective EF process [28, 29].

3.3. Effect of pH

The pH of the reaction system is an important operational parameter that significantly affects both the electrocoagulation (EC) and electro-Fenton (EF) processes. During the EC step, pH regulates the speciation and solubility of iron hydroxides, which directly influences the coagulation and adsorption mechanisms. Under near-neutral conditions (about pH 6–7), ferric hydroxide species, including $Fe(OH)_2$ and $Fe(OH)_3$, are primarily generated, facilitating ideal floc structures for pollutant removal by charge neutralization and sweep coagulation. At lower pH values, excessive acidity impedes floc formation by dissolving iron hydroxide precipitates, whereas at higher pH values, an excess of hydroxide ions may lead to anode passivation and decrease the rate of coagulant production [15, 30 - 31].

In the EF step, pH significantly influences the Fenton reaction process. In highly acidic conditions (pH 1-2), the quick breakdown of H_2O_2 and the intense rivalry between protons (H^+) and Fe^{2+} for reaction sites restrict the generation of •OH radicals, resulting in reduced oxidation efficiency. Conversely, as the solution becomes less acidic ($pH > 5$), Fe^{2+} ions are prone to precipitate as $Fe(OH)_3$, decreasing their solubility and consequently the catalytic sites necessary for •OH generation. Moreover, the stability of H_2O_2 reduces in alkaline environments, hence reducing the efficacy of the Fenton reaction[29, 34].

To evaluate the comprehensive impact of pH on the integrated EC/EF treatment system, four experiments were conducted at a constant current density of 40 mA/cm² and a H_2O_2 concentration of 0.5 g/L, with solution pH values set at 1, 3, 5, and 7. The highest COD removal (94.28%) occurred at pH 3, indicating the best equilibrium among Fe^{2+} solubility, floc stability, and hydroxyl radical (•OH) generating efficiency. Consequently, maintaining a pH of 3 promotes optimal electrochemical activity by retaining soluble Fe^{2+} species and boosting •OH radical production, thereby improving COD removal efficiency via the synergistic EC/EF process [33 - 37] . Figure 3 shows the influence of pH on COD removal efficiency in the EC/EF process at a current density of 40 mA/cm² and 0.5 g/L H_2O_2 addition. The optimal removal efficiency occurred at pH 3, indicating that acidic conditions promote hydroxyl radical production and improve the oxidation of organic contaminants.

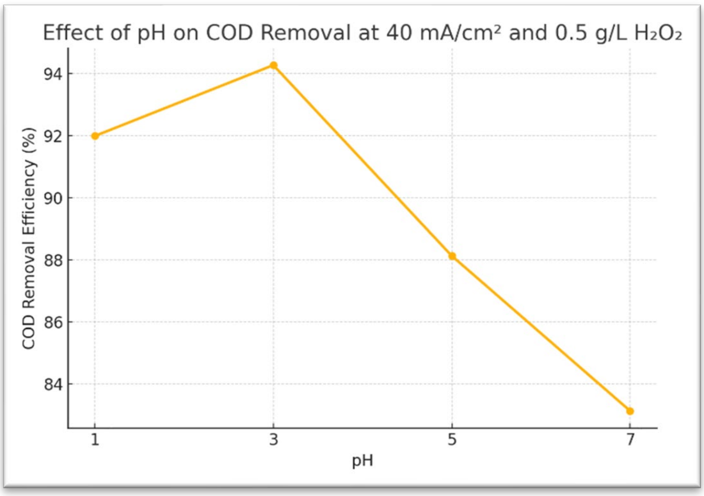

Figure 3. Effect of pH on COD removal efficiency during the EC/EF process at 40 mA/cm² and 0.5 g/L H_2O_2 addition.

4. Kinetic study

Understanding how pollutants break down is fundamental for elucidating the underlying mechanisms and enhancing the efficiency of electrochemical treatment processes. Kinetic modeling not only clarifies reaction pathways and rate-limiting steps but also enables the optimization of operational parameters to maximize pollutant removal performance [38-39]. This study examined the electrocoagulation (EC) process using four well-known kinetic models, including pseudo-first-order and pseudo-second-order. Applying these models provided deeper insights into pollutant destabilization and aggregation mechanisms, which are driven by the in-situ generation of coagulants from sacrificial iron electrodes [30 ,39-40] . Each model provides a distinct viewpoint on the surface contacts and transport mechanisms that regulate the EC step. In the electro-Fenton (EF) process, creating hydroxyl radicals (•OH) by the addition of hydrogen peroxide H_2O_2 and ferrous ions (Fe^{2+}) is crucial for breaking down organic pollutants; therefore, both pseudo-first-order and pseudo-second-order models were used to explain how the chemical oxygen demand (COD) is reduced [41-42]. The studies were conducted with different concentrations of hydrogen peroxide and different currents in order to evaluate their effect on the efficiency and overall rate of the reaction [26]. In the EC/EF sequential process, the efficiency of the EF process can be explained mechanically by the conditioning effect resulting after the completion of the electrocoagulation process, where the generated masses of $Fe(OH)_2$/$Fe(OH)_3$ generated in the EC process are absorbed by the phenols, colloids, and some free radicals present in the wastewater [15]. Removing them before the EF process reduces competition for (•OH) radicals, as they are consumed in large quantities during the free radical removal phase, which reduces the removal efficiency of the process [24,26]. In addition, the resistant organic molecules are destabilized and decomposed during the EC step, increasing their reactivity with •OH during the EF step. This provides a cleaner and more efficient medium for EF action, leading to greater free radical availability, improved reaction kinetics, and a higher COD removal rate compared to EF alone [17, 45].

4.1. Pseudo first order kinetics model of EC/EF

The pseudo-first-order kinetic model was employed to characterize the rate of COD removal in both the electrocoagulation (EC) and electro-Fenton (EF) processes. This model assumes that the rate of pollutant removal is exactly proportional to the concentration of residual pollutants in the solution. In the EC step, the differential form of the pseudo-first-order kinetic equation can be defined as:

$$\frac{dq_t}{dt} == k_1 \ (q_e - q_t) \tag{11}$$

Where:

q_t is the amount of COD removed at time t (mg/g),

q_e is the equilibrium amount of COD removed (mg/g),

k_1 (min^{-1}) is the pseudo-first-order rate constant for the EC process.

Upon integration between the limits t = 0 to t = t , the equation becomes:

$$\ln(q_e - q_t) = \ln(q_e) - k_1 \cdot t \tag{12}$$

A linear plot of $\ln(q_e - q_t)$ against t provides k_1 from the slope [46] . The higher correlation coefficients ($R^2 > 0.97$) observed at current densities of 20–50 mA/cm^2 indicate that COD removal during electrocoagulation follows pseudo-first-order kinetics. The rate constant k_1 increases with current density, due to an increase of the production of Fe^{2+} ions and coagulant species that facilitate the disintegration and aggregation of pollutants. These findings align with previous research indicating first-order behavior in EC processes, attributed to their reliance on contaminant concentration and electrochemical reaction rates [15, 46].

For the EF step, the pseudo-first-order kinetic model can be expressed in its differential form as:

$$\frac{dC_t}{dt} = -k_1 C_t \tag{13}$$

Integrating equation (13) between t = 0 and t = t yields:

$$\ln\left(\frac{C_o}{C_t}\right) = k_1 \cdot \mathrm{t} \tag{14}$$

Where k_1 (min^{-1}) is the rate constant for the EF process [48] . Linear regression analysis revealed robust correlation coefficients, indicating that COD removal during EF follows pseudo-first-order kinetics. This is mainly due to the formation of hydroxyl radicals (•OH) from the interaction between Fe^{2+} and H_2O_2, which facilitates the oxidation of organic materials. Comparable pseudo-first-order kinetic behavior in EF systems has been extensively reported, highlighting the reliance of reaction rate on the Fe^{2+}/H_2O_2 ratio and radical availability [34,38,47]. **Figure 4** shows the pseudo-first-order kinetic behavior of COD removal during the electrocoagulation (EC) process, showing that the plots of $\ln(q_e - q_t)$ versus time yield straight lines with high linearity, indicating that the reaction rate is effectively governed by first-order kinetics and increases with rising current density.

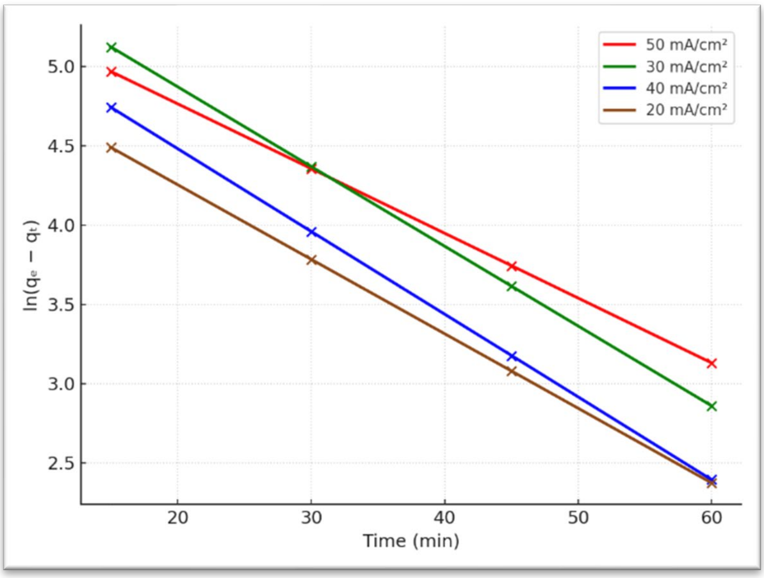

Figure 4. Pseudo first-order kinetic plots of **$\ln(q_e - q_t)$** versus **time** for COD removal during the electrocoagulation (**EC**) process at different current densities.

Figure 5 shows that COD removal during the electro-Fenton (EF) process follows pseudo-first-order kinetics, as shown by the linear correlation between $\ln(C_0/C_t)$ and time. Increasing the H_2O_2 concentration beyond 0.5 g/L resulted in a noticeable decline in the reaction rate, due to the scavenging effect of excess hydrogen peroxide, which consumes hydroxyl radicals (•OH) and consequently reduces the overall oxidation efficiency.

Figure 5. Pseudo first order kinetic plots of **ln**($\frac{C_0}{C_t}$) versus **time** for COD removal at **40 mA/cm²** during the electro-Fenton (**EF**) process at different H_2O_2 additions.

4.2. Second order kinetics model of EC/EF

The pseudo-second order kinetic model is widely applied to describe pollutant removal processes that are governed by chemisorption, where valence forces involve the sharing or exchange of electrons between adsorbent sites and target contaminants. In the electrocoagulation (EC) step, in situ-generated Fe^{2+} and $Fe(OH)_x$ species act as efficient coagulants [45, 48]. COD removal is attributed to their interaction with organic matter through surface complexation, precipitation, and enmeshment.

The differential form of the pseudo-second order equation is expressed as:

$$\frac{dqt}{dt} = k_2 (q_e - q_t)^2 \tag{15}$$

Where q_t is the amount of COD removed at time t (mg/g), q_e is the equilibrium COD removal (mg/g), and k_2 is the pseudo-second order rate constant (g·mg⁻¹·min⁻¹) [23]. After integration and linearization, the equation becomes:

$$\frac{t}{qt} = \frac{1}{(k_2 * qe^2)} + \frac{t}{qe} \tag{16}$$

A linear plot of t/qt against t shows if the COD removal conforms to this model [33]. This study indicates that COD removal data at all current densities (20–50 mA/cm²) align well with the pseudo-second order model, implying that chemisorption predominates the removal mechanism during electrocoagulation. Comparable findings have been documented in further electrocoagulation experiments concerning industrial effluents, wherein the removal of organic materials was effectively characterized by pseudo-second order kinetics [15,31,39]. In the EF step, a modified second-order kinetic model was employed to interpret the degradation behavior of COD, where C_t represents the amount of pollutant removed rather than the residual concentration in the solution. This model assumes that the reaction rate is governed by chemisorption mechanisms involving hydroxyl radical (•OH) interactions with refractory organics. The differential form of the model is given as:

$$\frac{dC_t}{dt} = K_2 \, (C_e - C_t)^2 \tag{17}$$

Integrating between the limits $C_t = 0$ at $t = 0$ and $C_t = C_t$ at time t gives:

$$\frac{t}{C_t} = \frac{1}{K_2 \, C_e^2} + \frac{t}{C_e} \tag{18}$$

This linear relationship between t/C_t and t enables the determination of the rate constant k_2 and the equilibrium concentration C_e from the slope and intercept, respectively. The good linearity obtained confirms that COD removal in the EF step follows the modified second-order kinetic model [31,50]. **Figure 6** shows that the pseudo-second order kinetic model provides a good linear correlation between t/q_t and time, indicating that COD removal during the electrocoagulation (EC) process is primarily governed by chemisorption mechanisms, with the reaction rate increasing as current density rises.

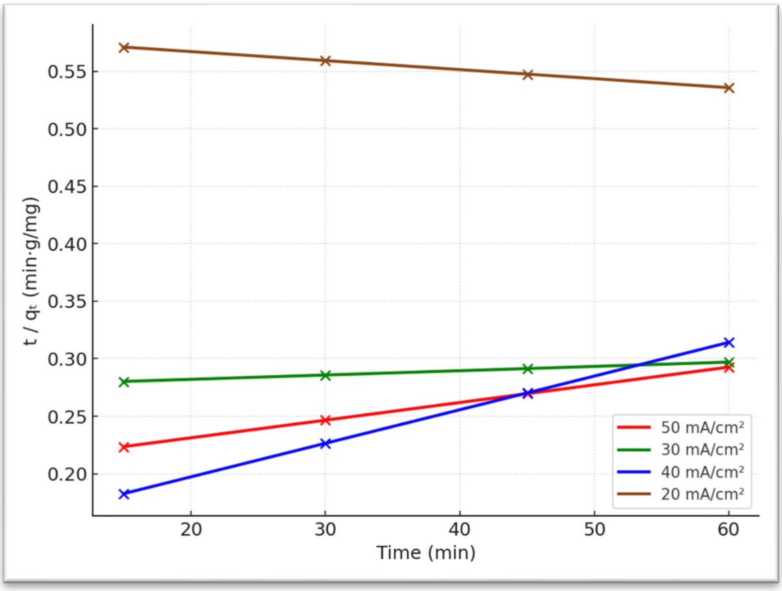

Figure 6. Pseudo-second order kinetic plot (**t/q_t** vs. **time**) for COD removal during the electrocoagulation (**EC**) process at different current densities.

Figure 7 shows that the modified second-order kinetic model provides a strong linear relationship between t/C_t and time, confirming that COD degradation during the electro-Fenton (EF) process follows second-order kinetics. The slope variation with H_2O_2 dosage indicates that excessive peroxide addition reduces efficiency due to hydroxyl radical scavenging at higher concentrations.

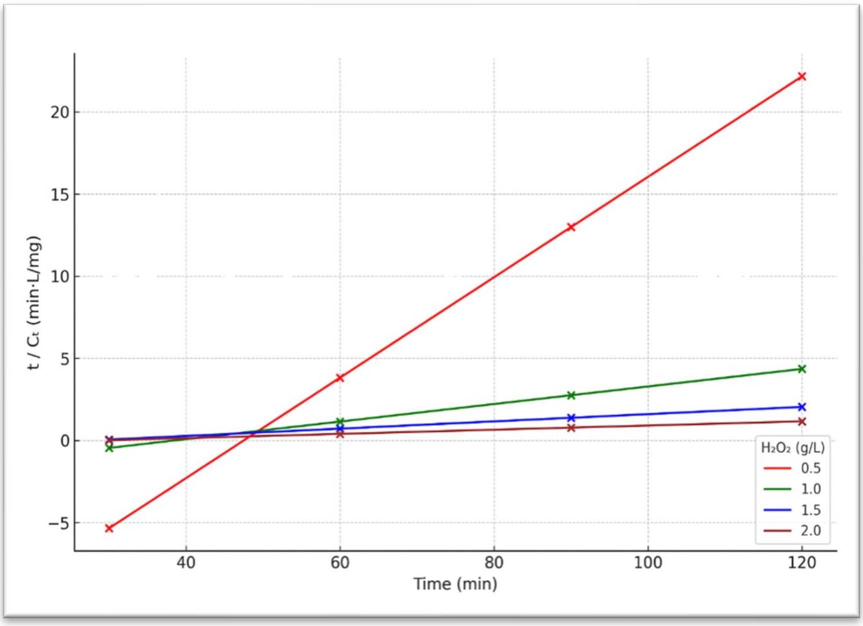

Figure 7. Second-order kinetic plots of **t/C_t** versus **time** for COD removal during the electro-Fenton (**EF**) process at different current densities.

Table 2 summarizes the kinetic rate constants (k_1 and k_2) obtained for both EC and EF processes under various current densities and H_2O_2 concentrations. The results reveal that both k_1 and k_2 values generally increase with current density, indicating enhanced pollutant removal due to higher Fe^{2+} generation and oxidizing radical formation, while excessive H_2O_2 concentrations (> 0.5 g/L) led to a decline in rate constants as a result of radical scavenging effects.

Table 3 . Kinetic rate constants (k_1 and k_2) for EC and EF processes at different H_2O_2 addition and current densities (pH = 7 for EC and pH = 3 for EF).

H_2O_2 Concentration (g/l)	**C.D (mA/cm^2)**	**Pseudo first order**		**Pseudo-second order**	
		Rate constant of EC (1/min)	**Rate constant of EF (1/min)**	**Rate constant of EC (1/mg·min)**	**Rate constant of EF (1/mg·min)**
0.5	20	0.002159	0.00936	0.00000744	0.010397
1	20	0.001856	0.00903	0. 00000016	0.006935
1.5	20	0.002043	0.01141	0.00001554	0.006082
2	20	0.001969	0.00879	0.00001015	0.004602
0.5	30	0.004491	0.01531	0.0000005	0.013469
1	30	0.004558	0.01642	0.00000202	0.017815
1.5	30	0.004633	0.01535	0.00000009	0.015934
2	30	0.004424	0.01268	0.00000034	0.007899
0.5	40	0.003913	0.04162	0.00018157	0.305558
1	40	0.004086	0.0225	0.00020977	0.053408
1.5	40	0.004369	0.01286	0.00021216	0.02209
2	40	0.004241	0.01416	0.00009840	0.012757
0.5	50	0.004596	0.03065	0.0001314	0.069434
1	50	0.0047	0.02212	0.00006008	0.034342
1.5	50	0.004347	0.0191	0.00019706	0.024465
2	50	0.004508	0.01962	0.00010928	0.008911

5. Sludge analysis

During the electrocoagulation process, when iron is used as a sacrificial electrode, it undergoes hydrolysis, forming iron hydroxides ($Fe(OH)_2$ and $Fe(OH)_3$). These hydroxides act as coagulants, binding and precipitating organic and inorganic pollutants present in wastewater. The accumulation of these hydroxides results in iron-rich sludge. Environmental concerns exist regarding EC, as this process produces iron-rich sludge. These concerns relate to phenols, hydrocarbons, and sulfide residues accumulating within the $Fe(OH)_3$/FeOOH matrix [15]. Research indicates that basic stabilization methods, including thermal conditioning and drying, or the integration of sludge into cementitious or ceramic materials, yield a cohesive, low-risk solid substance that markedly diminishes the mobility of pollutants [51] . Furthermore, the sludge generated in the EC process can be reused as a low-cost absorbent due to its high iron oxide content, thus allowing for its valorization rather than simply being treated as waste.

The EDS spectrum (**Figure 8**) derived from a representative sludge sample after the EC treatment verifies that the sludge predominantly comprises iron (67 wt%) and oxygen (30 wt%), suggesting the presence of iron oxyhydroxides such as $Fe(OH)_3$ and FeOOH. Trace amounts of chlorine (Cl) and sulfur (S) were identified, presumably stemming from leftover ions in the wastewater. Furthermore, trace elements like nickel (Ni), chromium (Cr), and copper (Cu) were detected, indicating that these metals were co-precipitated or adsorbed onto the surface of iron hydroxide flocs during the treatment process [18 ,52].

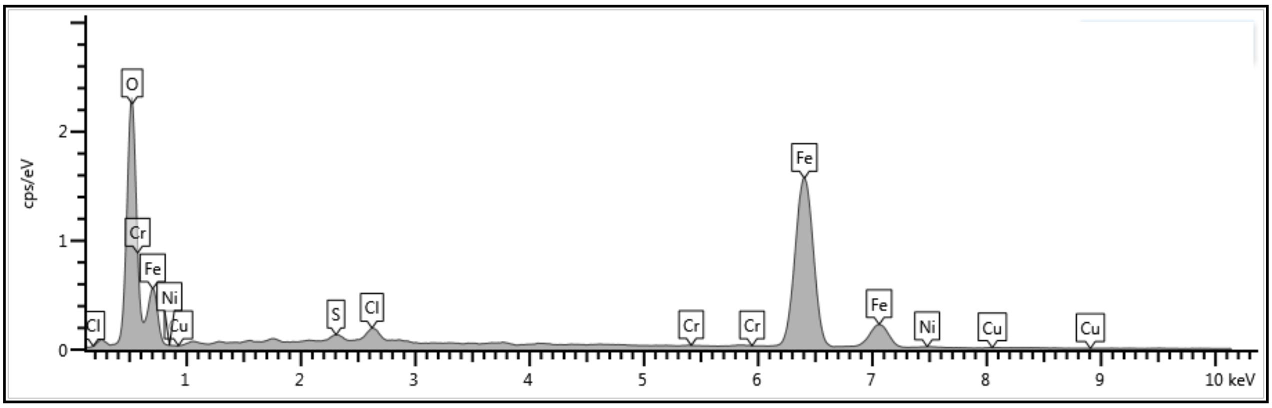

Figure 8. Energy Dispersive X-ray (EDS) spectrum showing the elemental composition of sludge generated after the EC process.

6. Economic evaluation

Energy consumption is a decisive factor in evaluating the sustainability and economic viability of electrochemical wastewater treatment technologies. It directly influences operating costs and determines whether large-scale implementation is feasible. In this study, the energy demand of both the electrocoagulation (EC) and electro-Fenton (EF) steps was carefully examined to assess the overall requirements of the sequential process. The results showed that energy consumption varied across operational conditions; for instance, experiment 9 exhibited a total energy usage of 3.359 kWh/m^3, reflecting the higher current density and extended EF duration. Such findings emphasize that while EC contributes to pollutant destabilization at moderate energy inputs, the EF step accounts for the majority of energy demand due to continuous hydroxyl radical generation [9, 16, 17].

These outcomes are consistent with previous work, where integrated EC/EF treatments demonstrated increased efficiency but also elevated energy consumption at higher current densities and longer treatment times [17, 44] . Consequently, optimizing operating parameters such as current density and H_2O_2 dosage is essential to balance pollutant removal efficiency with energy sustainability, making the sequential EC/EF approach both effective and economically competitive compared to conventional treatments[51, 53].

In this study the total energy used for the sequential electrocoagulation and electro-Fenton processes ranged from 1.94 to 10.34 kWh/m^3 across all 16 tests. These values are deemed appropriate for the electrochemical treatment of industrial wastewater and align with ranges documented in prior investigations [16,17]. The minimal energy requirements were observed at reduced current densities, specifically at 20 mA/cm^2; however, elevated intensities, such as 50 mA/cm^2, resulted in increased consumption. This pattern happens because higher currents create more coagulants and hydroxyl radicals, which help remove COD but also increase electrical energy use [9, 17] .

The comparative analysis reveals that the energy consumption numbers presented in this study are consistent with those in the existing literature. Reported values for textile wastewater treated with EC/EF ranged from 6.2 to 12.4 kWh/m^3 [16] , while lower ranges of 1.8 to 4.7 kWh/m^3 have been documented for surface water treated solely by electrocoagulation.[15].

The experiments done at 40 mA/cm^2 showed good results, achieving acceptable COD removal rates while using less than 4 kWh/m^3 of energy. These findings indicate that reduced current densities may provide more energy-efficient operational conditions for full-scale applications [17, 54].

The energy cost serves as an important economic indicator for assessing the viability of electrochemical wastewater treatment systems. It establishes a direct correlation between process performance and operational costs. The total energy cost (CE) was determined using the following equation:

$$C_E = E \times P \tag{19}$$

E is the electrical energy consumption (kWh/m^3), whereas P indicates the local electricity pricing (USD/kWh) [17]. The average industrial electricity pricing in Iraq, which is approximately 0.07 USD/kWh, was used to calculate the costs of the EC/EF operation in this study. The overall energy cost of the sequential EC/EF process varied between 0.14 and 0.72 USD/m^3, contingent upon the current density and treatment period. Aligning with findings from previous studies on the electrochemical treatment of industrial effluents [1, 2, 18, 55].

Notwithstanding the moderate rise in energy costs at elevated currents, the results acquired in this investigation stay within a plausible range when juxtaposed with traditional physicochemical methods. Furthermore, the measured COD removal efficiencies indicate that the EC/EF system maintains an advantageous equilibrium between energy use and pollutant removal, proving its appropriateness for sustainable and cost-effective wastewater treatment applications.

The expansion of EC/EF processes depends directly on the pollution behavior during the process, the durability of the electrodes used, the maintenance requirements, and the operating costs. During the gradual dissolution of anodes, layers may form during prolonged and continuous use, which can inhibit electrode efficiency. Graphite cathodes, on the other hand, accumulate iron hydroxide films and organic deposits, thus reducing the electrochemical activity of the process and necessitating electrode replacement or periodic maintenance [15]. Fouling is a critical issue in refinery wastewater, as the presence of substances such as suspended solids and oils can restrict free radical generation or even electron transfer, making it especially important to maintain surface integrity and cleanliness through proper use and periodic regeneration [1]. From an economic perspective, the loss of electrode efficiency and energy loss remain the two main factors contributing to the overall cost of the process. Thus, the electrodes' quality and efficiency must be improved, as well as the use of appropriate current densities and pH control during the EC or EF process. Also, the spacing between the electrodes is extremely important and very necessary to maintain satisfactory system performance and reduce potential costs in industrial environments [10, 17].

7. Conclusions

This study demonstrated the effectiveness of a sequential electrocoagulation (EC) followed by electro-Fenton (EF) process for the treatment of real refinery wastewater from the Najaf refinery. The integrated system exhibited excellent performance, achieving a maximum COD removal efficiency of 99.42% under optimal conditions of 40 mA/cm^2 current density and 0.5 g/L H_2O_2 dosage.

The key conclusions can be summarized as follows:

The pseudo first order kinetic model accurately described COD removal during both EC and EF steps, with correlation coefficients (R^2) consistently higher than 0.97, confirming the robustness of the model fit.

The highest rate constants (k) were obtained at current densities of 40–50 mA/cm^2, particularly when the applied H_2O_2 addition was maintained between 0.5 and 1.0 g/L.

1. The EF process operated most effectively at pH 3, which facilitated the generation of hydroxyl radicals (•OH) and significantly enhanced COD oxidation.
2. The sequential EC/EF process offers a technically viable and economically competitive treatment option for petroleum refinery wastewater, capable of achieving superior pollutant removal

efficiencies with moderate energy and chemical consumption. These findings highlight its strong potential for future scale-up and industrial applications.

3. The sequential EC/EF system attained a maximum COD removal efficiency of 99.42% under optimal conditions of 40 mA/cm² current density and 0.5 g/L H_2O_2 addition.
4. Due to the absence of energy-intensive ventilation units and the lower consumption of chemicals, the comparison indicated that the carbon footprint is lower in the EC/EF process than in conventional refinery treatment
5. The shift toward advanced nanostructured materials for ion-selective separation in membrane technologies (such as Li separation from wastewater and/or oil) parallels the ongoing need to integrate material-performance improvements in electrochemical treatment systems for complex wastewater matrices [56].

Conflict of interest

The authors declare no conflict of interest

References

1. M. S. Lawan, R. Kumar, J. Rashid, and M. A. E.-F. Barakat, "Recent advancements in the treatment of petroleum refinery wastewater," Water (Basel), vol. 15, no. 20, p. 3676, 2023.
2. T. K. C. Phu, P. L. Nguyen, and T. V. B. Phung, "Recent progress in highly effective electrocoagulation-coupled systems for advanced wastewater treatment," iScience, vol. 28, no. 3, 2025.
3. O. Akhavan, E. Hashemi, H. Zare, M. Shamsara, N. Taghavinia, and F. Heidari, "Influence of heavy nanocrystals on spermatozoa and fertility of mammals," Materials Science and Engineering: C, vol. 69, pp. 52–59, 2016, doi: https://doi.org/10.1016/j.msec.2016.06.055.
4. N. Rabiee et al., "Green porous benzamide-like nanomembranes for hazardous cations detection, separation, and concentration adjustment," J Hazard Mater, vol. 423, p. 127130, 2022.
5. A. M. Chávez et al., "Treatment of highly polluted industrial wastewater by means of sequential aerobic biological oxidation-ozone based AOPs," Chemical Engineering Journal, vol. 361, pp. 89–98, 2019.
6. X. Li, L. Fu, F. Chen, S. Zhao, J. Zhu, and C. Yin, "Application of heterogeneous catalytic ozonation in wastewater treatment: an overview," Catalysts, vol. 13, no. 2, p. 342, 2023.
7. L. S. Azmi, N. 'Ain Jabit, S. Ismail, K. E. H. Ku Ishak, and T. K. Abdullah, "Membrane filtration technologies for sustainable industrial wastewater treatment: a review of heavy metal removal.," Desalination Water Treat, vol. 323, p. 101321, 2025, doi: https://doi.org/10.1016/j.dwt.2025.101321.
8. P. Azik, "A review of international conventions regarding the responsibilities caused by oil pollution of the seas," Isagoge-J Humanit Soc Sci, vol. 3, no. 1, pp. 273–287, 2023.
9. Ö. Gökkuş, E. Brillas, and I. Sirés, "Sequential use of a continuous-flow electrocoagulation reactor and a (photo) electro-Fenton recirculation system for the treatment of Acid Brown 14 diazo dye," Science of the Total Environment, vol. 912, p. 169143, 2024.
10. H. Olvera-Vargas et al., "Challenges and opportunities for large-scale applications of the electro-Fenton process," Water Res, vol. 266, p. 122430, 2024.
11. L. E. Quispe Cardenas et al., "Electro-Fenton and induced electro-Fenton as versatile wastewater treatment processes for decontamination and nutrient removal without byproduct formation," ACS Es&t Engineering, vol. 3, no. 10, pp. 1547–1556, 2023.
12. E. Brillas, I. Sirés, and M. A. Oturan, "Electro-Fenton process and related electrochemical technologies based on Fenton's reaction chemistry," Chem Rev, vol. 109, no. 12, pp. 6570–6631, 2009.
13. B. M. Omar, M. A. Zyadah, M. Y. Ali, and M. A. El-Sonbati, "Pre-treatment of composite industrial wastewater by Fenton and electro-Fenton oxidation processes," Sci Rep, vol. 14, no. 1, p. 27906, 2024.
14. O. Akhavan, "Thickness dependent activity of nanostructured TiO2/α-Fe2O3 photocatalyst thin films," Appl Surf Sci, vol. 257, no. 5, pp. 1724–1728, 2010, doi: https://doi.org/10.1016/j.apsusc.2010.09.005.
15. J. N. Hakizimana et al., "Electrocoagulation process in water treatment: A review of electrocoagulation modeling approaches," Desalination, vol. 404, pp. 1–21, 2017, doi: https://doi.org/10.1016/j.desal.2016.10.011.
16. B. Louhichi, F. Gaied, K. Mansouri, and M. R. Jeday, "Treatment of textile industry effluents by Electro-Coagulation and Electro-Fenton processes using solar energy: A comparative study," Chemical Engineering Journal, vol. 427, p. 131735, 2022, doi: https://doi.org/10.1016/j.cej.2021.131735.
17. I. Dobrosz-Gómez, L.-M. Salazar-Sogamoso, J.-C. Castaño-Sánchez, D.-O. Salazar-López, and M.-Á. Gómez-García, "Environmental and Economic Evaluation of the Sequential Combination of Coagulation–Flocculation

with Different Electro-Fenton-Based Configurations for the Treatment of Raw Textile Wastewater," Water (Basel), vol. 16, no. 15, p. 2154, 2024.

18. Y. Mao, Y. Zhao, and S. Cotterill, "Examining current and future applications of electrocoagulation in wastewater treatment," Water (Basel), vol. 15, no. 8, p. 1455, 2023.
19. P. Agarwal, V. K. Sangal, and S. Mathur, "Sequential electro-coagulation and electro-Fenton processes for the treatment of textile wastewater," Water Environment Research, vol. 96, no. 9, p. e11118, 2024.
20. F. Azik, S. N. Mousavi, and B. Najafi, "The effects of granting subsidies to agricultural inputs on iranian households' welfare and environment by emphasis on computable general equilibrium model," Agricultural Marketing and Commercialization, vol. 5, no. 1, pp. 153–176, 2021.
21. M. Kobya, F. Ulu, U. Gebologlu, E. Demirbas, and M. S. Oncel, "Treatment of potable water containing low concentration of arsenic with electrocoagulation: Different connection modes and Fe–Al electrodes," Sep Purif Technol, vol. 77, no. 3, pp. 283–293, 2011.
22. F. Zhang et al., "High-efficiency electrosynthesis of hydrogen peroxide from oxygen reduction enabled by a tungsten single atom catalyst with unique terdentate N1O2 coordination," Adv Funct Mater, vol. 32, no. 16, p. 2110224, 2022.
23. J. S. Al-Marri, A. B. Abouedwan, M. I. Ahmad, and N. Bensalah, "Electrocoagulation using aluminum electrodes as a sustainable and economic method for the removal of kinetic hydrate inhibitor (polyvinyl pyrrolidone) from produced wastewaters," Frontiers in Water, vol. 5, p. 1305347, 2023.
24. F. Jean-M, D.-B. Xochitl, and S. Mika, "Towards reliable quantification of hydroxyl radicals in the Fenton reaction using chemical probes," RSC Adv, vol. 8, no. 10, pp. 5321–5330, 2018.
25. B. Louhichi, F. Gaied, K. Mansouri, and M. R. Jeday, "Treatment of textile industry effluents by Electro-Coagulation and Electro-Fenton processes using solar energy: A comparative study," Chemical Engineering Journal, vol. 427, p. 131735, 2022, doi: https://doi.org/10.1016/j.cej.2021.131735.
26. A. Akyol, O. T. Can, E. Demirbas, and M. Kobya, "A comparative study of electrocoagulation and electro-Fenton for treatment of wastewater from liquid organic fertilizer plant," Sep Purif Technol, vol. 112, pp. 11–19, 2013, doi: https://doi.org/10.1016/j.seppur.2013.03.036.
27. P. V. Nidheesh, R. Gandhimathi, and S. T. Ramesh, "Degradation of dyes from aqueous solution by Fenton processes: a review," Environmental Science and Pollution Research, vol. 20, no. 4, pp. 2099–2132, 2013.
28. I. Mohammed, H. H. Alwan, and A. N. Ghanim, "Using Box-Behnken experimental design for optimization of gas oil desulfurization by electrochemical oxidation technique," in IOP Conference Series: Materials Science and Engineering, IOP Publishing Ltd, Nov. 2020. doi: 10.1088/1757-899X/928/2/022158.
29. E. Neyens and Jjj. Baeyens, "A review of classic Fenton's peroxidation as an advanced oxidation technique," J Hazard Mater, vol. 98, no. 1–3, pp. 33–50, 2003.
30. M. C. Collivignarelli, R. Pedrazzani, S. Sorlini, A. Abbà, and G. Bertanza, "H2O2 based oxidation processes for the treatment of real high strength aqueous wastes," Sustainability, vol. 9, no. 2, p. 244, 2017.
31. E. Asgari, M. Aghanaghad, H. Nourmoradi, B. Hashemzadeh, and R. Aali, "Biodegradability enhancement and pre-treatment of industrial estate wastewater by electro-Fenton process," Desalination Water Treat, vol. 200, pp. 217–223, 2020.
32. W. Reátegui-Romero et al., "Effect of current density on COD removal efficiency for wastewater using the electrocoagulation process," Desalination Water Treat, vol. 184, pp. 15–29, 2020.
33. M. Ghahrchi, A. Rezaee, and A. Adibzadeh, "Study of kinetic models of olive oil mill wastewater treatment using electrocoagulation process. Desalination Water Treat 211: 123–130," 2021.
34. I. A. Katsoyiannis, T. Ruettimann, and S. J. Hug, "pH dependence of Fenton reagent generation and As (III) oxidation and removal by corrosion of zero valent iron in aerated water," Environ Sci Technol, vol. 42, no. 19, pp. 7424–7430, 2008.
35. Y. Wang, H. Li, and L. Ren, "Organic matter removal from mother liquor of gas field wastewater by electro-Fenton process with the addition of H2O2: effect of initial pH," R Soc Open Sci, vol. 6, no. 12, p. 191304, 2019.
36. M. Ayoub, "Fenton process for the treatment of wastewater effluent from the edible oil industry," Water Science & Technology, vol. 86, no. 6, pp. 1388–1401, 2022.
37. C. A. Gómez, M.-Á. Gómez-García, and I. Dobrosz-Gómez, "Analysis of the capacity of the Fenton process for the treatment of polluted wastewater from the leather dyeing industry," The Scientific World Journal, vol. 2023, no. 1, p. 4724606, 2023.
38. K. R. Minnalkodi Senguttuvan, K. Sellappa, and S. Kuppusamy, "Performance Evaluation of the Electro-Fenton Process for Distillery Wastewater Treatment," Sustainability, vol. 16, no. 15, p. 6512, 2024.
39. E. Pasciucco, F. Pasciucco, R. Iannelli, and I. Pecorini, "A Fenton-based approach at neutral and un-conditioned pH for recalcitrant COD removal in tannery wastewater: Experimental test and sludge characterization," Science of the Total Environment, vol. 926, p. 172070, 2024.
40. M. Issa, D. Haupt, T. Muddemann, U. Kunz, and M. Sievers, "The Electrochemical Reaction Kinetics during Synthetic Wastewater Treatment Using a Reactor with Boron-Doped Diamond Anode and Gas Diffusion Cathode," Water (Basel), vol. 14, no. 22, p. 3592, 2022.

41. K. Bani-Melhem et al., “On the performance of electrocoagulation treatment of high-loaded gray water: kinetic modeling and parameters optimization via response surface methodology,” Appl Water Sci, vol. 15, no. 5, pp. 1–21, 2025.
42. N. S. Graça and A. E. Rodrigues, “The combined implementation of electrocoagulation and adsorption processes for the treatment of wastewaters,” Clean Technologies, vol. 4, no. 4, pp. 1020–1053, 2022.
43. G. F. Khaleel, I. Ismail, and A. H. Abbar, “Kinetic modeling of a solar photo-electro-Fenton process for treating petroleum refinery wastewater,” Case Studies in Chemical and Environmental Engineering, vol. 8, p. 100460, 2023.
44. A. Kundu, N. Gupta, and A. S. Kalamdhad, “Optimization and kinetic analysis of electrocoagulation-assisted adsorption for treatment of young landfill leachate,” J Environ Manage, vol. 366, p. 121779, 2024, doi: https://doi.org/10.1016/j.jenvman.2024.121779.
45. B. Louhichi, F. Gaied, K. Mansouri, and M. R. Jeday, “Treatment of textile industry effluents by Electro-Coagulation and Electro-Fenton processes using solar energy: A comparative study,” Chemical Engineering Journal, vol. 427, p. 131735, 2022, doi: https://doi.org/10.1016/j.cej.2021.131735.
46. M. Ghahrchi, A. Rezaee, and A. Adibzadeh, “Study of kinetic models of olive oil mill wastewater treatment using electrocoagulation process,” Desalination Water Treat, vol. 211, pp. 123–130, 2021, doi: https://doi.org/10.5004/dwt.2021.26516.
47. I. Mohammed, H. H. Alwan, and A. N. Ghanim, “Study reaction kinetics of fuel model desulfurization by electrochemical oxidation technique,” Al-Qadisiyah. J. Eng. Sci., vol. 14, pp. 1–5, 2021.
48. E. Brillas and C. A. Martínez-Huitle, “Decontamination of wastewaters containing synthetic organic dyes by electrochemical methods. An updated review,” Appl Catal B, vol. 166–167, pp. 603–643, 2015, doi: https://doi.org/10.1016/j.apcatb.2014.11.016.
49. K. S. Bharathi and S. T. Ramesh, “Removal of dyes using agricultural waste as low-cost adsorbents: a review,” Appl Water Sci, vol. 3, no. 4, pp. 773–790, 2013, doi: 10.1007/s13201-013-0117-y.
50. Y. S. Ho and G. McKay, “Pseudo-second order model for sorption processes,” Process Biochemistry, vol. 34, no. 5, pp. 451–465, 1999, doi: https://doi.org/10.1016/S0032-9592(98)00112-5.
51. M. A. Aljaleel and H. H. Alwan, “Modeling the Effect of Operation Variables on Copper Ions Removal by Electrocoagulation,” in 2022 2nd International Conference on Advances in Engineering Science and Technology (AEST), 2022, pp. 111–115. doi: 10.1109/AEST55805.2022.10413162.
52. P. V Nidheesh, B. Behera, D. S. Babu, J. Scaria, and M. S. Kumar, “Mixed industrial wastewater treatment by the combination of heterogeneous electro-Fenton and electrocoagulation processes,” Chemosphere, vol. 290, p. 133348, 2022, doi: https://doi.org/10.1016/j.chemosphere.2021.133348.
53. C. Barrera-Díaz et al., “Electrochemical Advanced Oxidation Processes: An Overview of the Current Applications to Actual Industrial Effluents,” 2014.
54. K. Quispe-Ramos et al., “Energy-Efficient Coaxial Electrocoagulation for Integrated Treatment of Urban Wastewater and Acid Mine Drainage: A Response-Surface Approach,” Applied Sciences, vol. 15, no. 19, p. 10452, Sep. 2025, doi: 10.3390/app151910452.
55. F. Al-Ajmi, M. Al-Marri, and F. Almomani, “Electrocoagulation Process as an Efficient Method for the Treatment of Produced Water Treatment for Possible Recycling and Reuse,” Water (Switzerland), vol. 17, no. 1, Jan. 2025, doi: 10.3390/w17010023.
56. R. Rahighi et al., “Two-dimensional materials in enhancement of membrane-based lithium recovery from metallic-ions-rich wastewaters: A review,” Desalination, vol. 543, p. 116096, 2022, doi: https://doi.org/10.1016/j.desal.2022.116096.